

SEA SURFACE CONDITION IN THE BAY OF BENGAL
SINCE THE EARLY PLIOCENE

A Thesis submitted to the faculty of
San Francisco State University
In partial fulfillment of
the requirements for
the Degree

Master of Science

In

Geoscience

by

Drew Alexander Lowdermilk

San Francisco, California

August 2020

Copyright by
Drew Alexander Lowdermilk
2020

CERTIFICATION OF APPROVAL

I certify that I have read *Sea Surface Conditions in the Bay of Bengal since the Early Pliocene* by Drew Alexander Lowdermilk, and that in my opinion this work meets the criteria for approving a thesis submitted in partial fulfillment of the requirement for the degree Master of Science in Geoscience at San Francisco State University.



Petra Dekens, Ph.D.
Professor



Lyndsey Fox, Ph.D.
Professor



Alexander Stine, Ph.D.
Associate Professor

SEA SURFACE CONDITION IN THE BAY OF BENGAL
SINCE THE EARLY PLIOCENE

Drew Alexander Lowdermilk
San Francisco, California
2020

Modern CO₂ concentrations have reached 410 ppm, and there is considerable uncertainty about how climate change will affect the variability and intensity of the Asian Monsoon System (AMS). We can improve our understanding by studying how the Indian Ocean and the AMS responded to past climate change. Although the early Pliocene is not a perfect analogue for future warming, it is the most recent time in earth history when CO₂ concentrations were higher than today, and global average temperature was 3-4°C warmer. SST in the Atlantic & Pacific Ocean were 3-7°C higher in the eastern basins and remained stable in the Indo-Pacific warm pool. There is little data from the Indian Ocean through the last 6 Ma, limiting our understanding of how the monsoon and ocean circulation have changed. We generated foraminifera paleoclimate records from IODP Site U1451 (8°N, 88°E in 3607m water depth) in the Bay of Bengal. The top 200 m of Site U1451 is mostly calcareous clay, and a preliminary age model indicates this interval represents the last 6 Ma. We picked ~30 *T. sacculifer* with samples spaced at 40 cm. Mg/Ca of *T. sacculifer* was measured and converted to SST using multiple published calibrations. SST using the Dekens et al., 2002, carbonate dissolution corrected calibration at Site U1451 ranges from 26-30°C, well within the range to support the atmospheric convection required to support the AMS. There appears to be no long-term cooling trend through the past ~3 Ma. This new Bay of Bengal record is similar to those from ODP Site 758 in the Indian Ocean and ODP Site 806 in the western Pacific warm pool, which record a similar SST range and long-term features in SSTs in the past ~3 Ma.

I certify that the Abstract is a correct representation of the content of this thesis.


Chair, Thesis Committee


Date

ACKNOWLEDGEMENTS

I thank and acknowledge my advisor, Dr. Petra Dekens, and my committee members, Dr. Alexander Stine and Dr. Lyndsey Fox, for their guidance, support, and contributions to this study. I am indebted to the IODP Expedition 354 team, as this study would not have been possible without their collection and initial processing of the core samples. I also acknowledge the members of the UC Santa Cruz Institute of Marine Science's Marine Analytical Laboratory for their invaluable assistance, as well as the facilities and instruments utilized for sample cleaning and analysis. In addition, I would like to thank the John A. and Anna P. Monteverdi Fellowship, CoSE, and the Department of Earth & Climate Sciences for their financial support during my graduate studies. Finally, I thank my wife for her unwavering support. I am forever grateful to all that have assisted in some capacity.

TABLE OF CONTENTS

List of Table	vii
List of Figures.....	viii
List of Appendices.....	ix
Introduction	1
Background.....	4
Method.....	7
Results	10
Age Model	10
Foraminifera Mg/Ca	11
Mg/Ca Calibration	12
Discussion.....	15
Paleoceanographic reconstruction in sediment fan environments	16
SST records	18
Implications for the presence of AMS	20
Implications for the Indo-Pacific Warm Pool dynamics	22
Conclusions	25
Reference.....	26
Appendices	35

LIST OF TABLES

Table	Page
1. Pliocene Age Model.....	38
2. Mg/Ca Calibrated SSTs at Site U1451.....	39
3. Pliocene – Present Tropical SSTs.....	40

LIST OF FIGURES

Figures	Page
1. Bay of Bengal Map.....	41
2. Bay of Bengal SSTs Map.....	42
3. Core U1451A Characteristics.....	43
4. Age Model.....	44
5. <i>T. sacculifer</i> Mg/Ca.....	45
6. <i>T. sacculifer</i> Mn/Ca.....	46
7. SST Record (multiple calibrations).....	47
8. Bay of Bengal SSTs Record.....	48
9. Indo-Pacific Warm Pool SST Comparison.....	49
10. Eastern Equatorial Pacific SST Comparison.....	50

LIST OF APPENDICES

Appendix	Page
1. <i>T. sacculifer</i> taxonomic identification.....	35
2. Cleaning Procedures.....	35
3. Mn/Ca values.....	37

INTRODUCTION

Modern global warming is driven by increases in atmospheric CO₂ concentrations, which have increased to levels (410 ppm; IPCC, 2014) that Earth's climate system has not experienced since the early Pliocene (~4-5 Ma). Global temperatures have increased by 0.85°C (0.65 to 1.06°C) over the last ~150 years and are projected to increase by 2-4°C degrees by 2100 (IPCC, 2014). The Earth's surface is 70% ocean, and it is here that the increased radiation is predominantly absorbed. The patterns of sea surface temperature (SST) distribution have a profound effect on heat transport and regional and global climate. For example, average global temperatures increase during El Niño years, due to regional changes in the SST pattern across the equatorial Pacific Ocean (Quinn et al., 1987).

Understanding climate and ocean dynamics in the past can provide critical insight for predicting the future impacts of a warmer world. Because ocean temperatures have an important impact on regional and global climate, there has been an effort to reconstruct ocean conditions during previous times of global warmth (Fedorov et al., 2013). The Pliocene (2.6 – 5.3 Ma) is the most recent time in Earth history when the global climate sustained (for ~2 Ma) temperatures warmer than today (Fedorov et al., 2013). The Pliocene had analogous atmospheric CO₂ concentrations to today (~400 ppm) (Stap et al., 2016; Raymo et al., 1996). However, the global climate during this epoch was much

different than our modern climate, and average global surface temperature was 3-4°C warmer than today (Brierley et al., 2015). This is significantly warmer than what climate models predict with this level of CO₂ (Fedorov et al., 2013).

The early to mid-Pliocene (3.5 – 5.3 Ma) was warmer and more stable than our modern climate (Fedorov et al., 2013). The meridional and zonal temperature SST gradients were smaller during the early Pliocene compared to today (Fedorov et al., 2013). This is a result of warmer SSTs normally found in the western tropical basins extending into the eastern tropics and subtropics of the Pacific and Atlantic basins as well as toward the poles (Brierley and Fedorov, 2010). SST in the eastern equatorial Pacific were 4-6°C warmer in the early Pliocene compared to today (Fedorov et al., 2013), while western equatorial Pacific warm pool SST remained relatively stable (~29-30°C) since the Pliocene (Fedorov et al., 2013; Wara et al., 2005). The SST structure in the Pacific during the Pliocene represents a climatic regime is often referred to as El Padre, for its resemblance to an El Niño event (Ford et al. 2015). However, unlike an El Niño, which is a short-term climate oscillation (2-7 yrs), the early Pliocene El Padre was a shift in the mean background climate state (Ford et al., 2015). Similar to an El Niño, warmer temperatures penetrated into the subsurface, deepening the thermocline across the tropical Pacific during the Pliocene (Ford et al., 2015). Subsurface temperatures in the Eastern Equatorial Pacific cold tongue were ~10°C warmer during the early Pliocene (Ford et al. 2012).

Efforts to reconstruct paleoceanographic conditions through the Pliocene have been concentrated in the Atlantic & Pacific Ocean basins, while there are few records in the Indian Ocean (Fedorov et al., 2013). Of the three Pliocene records in the Indian Ocean (Fedorov et al., 2013), only one has data from the late Pliocene to present (Herbert et al., 2010). However, this record is the coastal waters of the northern Arabian Sea where upwelling activity contributes to the variance in SST (Herbert et al., 2010). The remaining two records span the Pliocene (2.5 – 5 Ma) but fail to capture the climate evolution from Pliocene to present (Karas et al., 2009; Karas et al., 2011). Existing records in the Indian Ocean fail to highlight the broader Indian Ocean.

Sediment cores from the Bay of Bengal (Figure 1) present an opportunity to investigate connections between regional climate, tectonics, and oceanographic processes. Creating a paleoceanographic reconstruction in the southern Bay of Bengal allows us to examine connections between the tropical Indian Ocean and northern monsoon system, and provide insight to the broader Indian Ocean Pliocene/Pleistocene climate evolution (Clemens et al. 2015; France-lanord et al. 2015). IODP Expedition 354 drilled seven sites along 8°N. The sites are perpendicular to the path of the modern seasonal Summer Monsoon Current (Figure 2; Schott et al., 2009), which carries warm seawater from the tropical ocean into the northern Indian Ocean. The seasonal influx of warm SSTs, along with other atmospheric processes, create and sustain the Asian Monsoon System (AMS), which are responsible for 1-4 meters of annual precipitation over the lesser and greater Himalayas (Burbank et al, 2003).

This study focuses on the sediment cores drilled during Expedition 354 to generate paleoceanographic reconstructions that will improve our understanding of the link between the warm tropical Indian Ocean and the critical regional processes in the northern Bay of Bengal. The eastern most site of Expedition 354, Site U1451 (8°0.42'N, 88°44.50'E in 3607.3 m water depth), was cored with the intention of reaching the oldest parts of the Bengal Fan (France-Lanord et al., 2015). Site U1451 is far enough from the modern active channel to contain well preserved hemipelagic layers of calcareous, microfossil rich clay within the top ~200 meters of the core (Figure 3; France-Lanord et al., 2016). Mg/Ca analysis of *Trilobatus sacculifer*, a planktonic species of foraminifera, will be used to generate SSTs through the last 5 Ma. These records will allow us to understand how the southern Bay of Bengal, and the Indian Ocean more broadly, has responded to global climate change since the early Pliocene.

BACKGROUND

In the Bay of Bengal, one main source of sedimentation is from the turbidity currents that episodically transport terrigenous sediment from the continental shelf out into the bay (Figure 1; Weber et al., 2003). These currents incise channels into the Bengal Fan where the majority of sedimentation occurs in overspill channel banks onto inner bends, establishing a channel-levee system (Figure 1; Curray et al., 2003). Pelagic sediments in this depositional environment are most likely mixed with transported

transport terrigenous sediments (France-Lanord et al., 2015). At locations distant from an active channel, the predominant sedimentation is hemipelagic which includes the calcareous shells of planktonic foraminifera. Studies of the channel-levee system in the Bay of Bengal have shown that foraminifera along an active channel could have originated at some distal location further north (Fritz-Endres & Dekens, 2019). The study used the core top samples from three locations to show that levee deposits are a mix of those from the overlying water column and from locations further upstream of the active channel (Fritz-Endres & Dekens, 2019). This same study showed that foraminifera from the hemipelagic layers of a sediment core reliably record the overlying condition of the water column (Fritz-Endres & Dekens, 2019).

Foraminifera are single-celled marine organisms whose shells are composed of calcium carbonate (CaCO_3) and are abundant all over the ocean. The geochemistry of the shells of foraminifera record the conditions of ocean water, such as SST and sea surface salinity (SSS), in which they were formed (Boyle et al., 1981; Delaney et al., 1985). Foraminifera use calcium (Ca^{2+}) when constructing their shells, but other cations such as magnesium (Mg^{2+}) substitute for calcium at a ratio that is an exponential function of the temperature of the water in which it was constructed (Elderfield & Ganssen, 2000). The warmer the ocean temperature the more magnesium is incorporated (Elderfield & Ganssen, 2000). To create a paleoceanographic reconstruction in the Bay of Bengal we will use Mg/Ca ratios from planktonic foraminifer over the last 6 Ma.

Although Mg/Ca is a widely used SST proxy, there are several potential biases that must be considered. The Mg/Ca concentration of a foraminifer is susceptible to contamination from clays, organic material, metal oxides, and laboratory supplies. Contamination could lead to a higher Mg/Ca ratio and an overestimate of the temperature of the water in which the shell was formed (Boyle & Keigwin, 1985; Elderfield et al., 2006). We followed well established cleaning procedures and lab protocols to minimize any contamination that could lead to a Mg/Ca bias (Barker et al., 2003), and tested for contamination by measuring Mn/Ca as a contamination indicator (see results).

When the deep ocean is undersaturated with respect to calcite, the foraminifera will undergo partial dissolution as they sink through the water column and lay at the sediment/water interface (before burial). Partial dissolution dissolves the magnesium-rich calcite of foraminifera's shell preferentially, which lowers the Mg/Ca and causes a cold temperature estimate bias (Dekens et al., 2002; Anand et al., 2003). Calcite dissolution increases with depth due to the pressure effects on the calcite solubility constant. Multiple calibration equations exist to convert the Mg/Ca concentration to SST (Dekens et al., 2002; Anand et al., 2003), and some calibrations include corrections for biases associated with dissolution (Dekens et al., 2002; Regenberg et al., 2006). The anticipated calibration method chosen will account for the positive, exponential relationship between Mg/Ca concentration and temperature, the specific species of foraminifera, and the effects of preferential dissolution.

METHODS

The lithology of the top 200 meters of core U1451 shows that this interval consists of mostly foraminifera-rich hemipelagic calcareous clay with intermittent sandy turbidites (Figure 3; France-Lanord et al., 2015). We collected 221 20mL samples from the top 170 meters of hole U1451A (cores 1H – 27H). Samples were taken every 0.4 meters in calcareous clay sections, but no samples were collected in the sandy turbidite sections. The sampling density was greatest in calcareous clay sections because there is a greater likelihood of finding fossilized foraminifera with origins from the overlying water column.

Individual samples were placed in a 500 mL Nalgene bottle and filled with approximately 150 mL DI water. The bottles were placed on a shake table for 48 hours to one week to disaggregate the sediment. Each sample was wet sieved to separate the clay (<0.63 μm) from the larger size fraction containing the foraminifera. The > 0.63 μm fraction was oven dried at 45°C then sieved into two size fractions, 250-355 μm and the 355-425 μm . It is preferential to have foraminifera from the larger, 355-425 μm , size fraction, as these planktonic foraminifera more accurately record surface water conditions (Spero & Lea, 1996).

Each size fraction was examined under a microscope to identify and pick *Trilobatus sacculifer*, *Globigerinoides ruber*, and *Globorotalia tumida* for analysis (Appendix 1). Juvenile *T. sacculifer* live within the photic zone where they can obtain their required amount of light and food (Bé et al., 1982). Juvenile *T. sacculifer* were preferentially selected because during the adult stage *T. sacculifer* migrate deeper, grow a characteristic sac-like chamber as well as gametogenic calcite, inhibiting the shells use as a geochemical proxy (Bé et al., 1982; Brummer et al., 1986). *G. tumida* spends its life at 70 - 120 meters below the sea surface, at the bottom of the photic zone (Ravelo & Fairbanks, 1992). This ecological characteristic makes the shell chemistry of the *G. tumida* useful for identifying trends in the thermocline. *G. ruber* live at the top of the water column (0-50 m), recording sea surface conditions (Hemleben et al., 1989; Farmer et al., 2007).

Approximately 60 individual foraminifera of each species were picked from each size fraction where possible. Mg/Ca analysis requires 200 to 600 μg of calcite. Foraminifera from each sample were weighed on a Sartorius CP2P microbalance (0.001 mg readability and 0.003 mg repeatability). The samples were gently cracked between two pieces of cleaned glass plates while being examined under microscope to ensure the samples were not crushed. The shell fragments were mixed to homogenize the sample and then split into three separate aliquots; two for Mg/Ca replicates and one for $\delta^{18}\text{O}$ analysis. Measuring Mg/Ca on splits reduces the influence of individual shell bias, an idea of our precision when cleaning samples, and a reserve if a sample is lost during

cleaning or analysis process. Mg/Ca samples were divided into two splits (300-500 μg) if the sample was large enough. Relative abundance of foraminifera decreased downcore. Most Pleistocene samples possessed adequate numbers of foraminifera for Mg/Ca, $\delta^{18}\text{O}$ analysis, and provide replicates. Most Pliocene samples had too few foraminifera for a single Mg/Ca analysis. However, preservation of foraminifera remained consistent throughout the core.

We followed the Mg/Ca cleaning methods first established by Boyle & Keigwin (1985) to remove organics originally trapped within the shells and reduce uncertainty due to magnesium contamination by stripping potential manganese carbonate overgrowth (Barker et al., 2003; Boyle & Keigwin, 1985). The process includes an initial set of rinses with ultra-pure (Milli-Q) deionized water and methanol, oxidative and reductive steps, followed by a heat rinse, and a weak acid leach. A full recounting of the cleaning procedures can be found in Appendix 2.

The cleaned samples were analyzed on an Inductively Coupled Plasma Optical Emission Spectrometer (ICP-OES) at the at the UC Santa Cruz Marine Analytical Lab. A known liquid consistency standard (FLCS-2) was run after every 10 samples to measure the accuracy of the ICP-OES output. The long-term ICP-OES precision of the FLCS, from all runs performed by our lab at the UC Santa Cruz Marine Analytical Lab since 2015, has a standard deviation of 0.014 mmol/mol. This is an indication of accurate measurements of Mg/Ca ratios. Additionally, to evaluate the consistency of our cleaning a *T. sacculifer* and *G. crassiformis* standard were cleaned and run every 28 samples. The

G. crassiformis standard had a standard deviation of 0.12 mmol/mol (0.36°C). The *T. sacculifer* standard had a standard deviation of 0.08 mmol/mol (0.24°C).

RESULTS

Age model

A preliminary age model was constructed for Site U1451 using ten magnetic reversals within the top 200 meters of core 1451A as tie points (Table 1; Figure 4). We assumed constant sedimentation rates between tie points and converted meters below the seafloor to age. The data range from the present to the late Pliocene (0-3.2 Ma). In the future, a more robust age model for Site U1451 will be constructed by comparing a local benthic $\delta^{18}\text{O}$ record using *Uvigerina peregrina* with the LR04 global benthic $\delta^{18}\text{O}$ stack in intervals where there the sedimentation rates are relatively high (Lisiecki & Raymo, 2005). Our first magnetic reversal within the existing age model appears at 72.24 meters (0.781 Ma). The top 80 meters of core 1451A is dominated by terrigenous sand deposits likely from turbidity currents (Frances-Lanord et al., 2015). The sedimentation rate during this period was likely episodic, meaning it's unlikely that sediment was deposited at a constant rate for ~1 Ma (Frances-Lanord et al., 2015). Deeper in the core (80-180m) the dominate sediment becomes hemi-pelagic calcareous clay. Within these deeper sections of the core we see increases in the capturing of magnetic reversals, which provides an increase in the age model resolution. We are most confident in the relatively

constant sedimentation from 70-85 and 130- 170m.

Foraminifera Mg/Ca

We use Mg/Ca of *T. sacculifer* to reconstruct SST. *T. sacculifer* Mg/Ca values range from 2.71 – 4.16 mmol/mol (Figure 5) with an average of 3.43 mmol/mol. Despite the gaps in our record there is no evidence of a long-term trend in the Mg/Ca ratios (Figure 5).

A potential source of bias when using the Mg/Ca ratio of shell calcite is magnesium contamination from organics, clays, and metal oxides. Magnesium contamination would lead to higher Mg/Ca values and an overestimate of SSTs, so it is essential to test for a contamination prior to converting to SSTs (Barker et al., 2003; Boyle, 1983). The Mn/Ca ratio is a common test for exposure to magnesium contamination as increased levels of Mn/Ca values are a good indicator of magnesium contamination from organics and clays (Boyle and Keigwin, 1985; Barker et al., 2003). Additionally, the Mn/Ca analysis addresses the issue of manganese carbonate overcoating that may not have been entirely removed during the cleaning process (Boyle, 1983; Barker et al., 2003). Our cleaning methods included a reductive step that is designed to remove the manganese carbonate overcoating (Barker et al., 2003).

The Mn/Ca values of our samples range from 0.007 - 1.472 with an average of 0.96 mmol/mol (Figure 6). These Mn/Ca values are higher than the typical range for oxidative-reductive cleaning methodology (Barker et al., 2003). However, there is no correlation between Mn/Ca and Mg/Ca ($r^2 = \sim 0.2$; Figure 6) indicating the higher Mn/Ca values were not a result of manganese carbonate overcoatings. Other studies focusing on the Pliocene and using similar methodology noted high Mn/Ca values ($>100 \mu\text{mol}$) in their samples (Wara et al., 2005; White & Ravelo, 2020; Barker et al., 2003). These studies reported an average Mn/Ca values greater than 1 mmol/mol, significantly greater than $100 \mu\text{mol}$, and in both cases their data showed little to no correlation between Mn/Ca and Mg/Ca values (Wara et al., 2005; White & Ravelo, 2020). We conclude that samples with high Mn/Ca values ($>100 \mu\text{mol}$) from Site U1451 accurately represent the Mg/Ca signal and can be used to reconstruct SST.

Mg/Ca calibrations

We converted Mg/Ca values to SST estimates using published calibrations that convert Mg/Ca to SST based on an exponential relationship between the Mg/Ca ratio of shell calcite and the temperature of the water in which it was formed (Anand et al., 2003; Dekens et al., 2002; Regenberg et al., 2006). The widely used Anand et al., 2003, calibration is based on twelve species of planktonic foraminifera collected from sediment traps where the samples were not subject to dissolution. The calibration is species

specific, and we used the calibration for *T. sacculifer* samples the 350-500 μm size fraction,

$$\text{Mg/Ca} = 0.38 \exp(0.090T)$$

SST estimates using the Anand et al., 2003 calibration range from $\sim 22\text{-}26^\circ\text{C}$ with an average temperature of 24.4°C , which is significantly lower than the modern average SST of $29 \pm 0.8^\circ\text{C}$ (Levitus, 1982).

Three dissolution corrected calibrations were used to convert Mg/Ca values to SSTs. These calibrations were all based on analyses of core top samples, which have undergone varying amounts of dissolution. Using modern core tops, these studies developed relationships between Mg/Ca, SST, and preservation. The Dekens et al., 2002 used core top samples from both the tropical Pacific and Atlantic basins. Two approaches were used in the species-specific calibrations. One dissolution correction uses the core depth as a proxy for preservation, but this requires an offset between Atlantic and Pacific core tops because Pacific deep water is older and therefore has lower CO_3^{2-} concentration. Although Site U1451 is in the Indian Ocean the calibration for the Pacific basin was chosen:

$$\text{Mg/Ca} = 0.37 \exp 0.09[T - 0.36(\text{core depth km})]$$

There is no core-depth corrected calibration for the Indian Ocean, and although the Indian Ocean and Pacific basin exchange waters and have relatively old deep water in comparison to the Atlantic, this lack of core tops from the Indian Ocean could lead to a

less accurate dissolution correction. However, the ΔCO_3^{2-} at the western equatorial Pacific (ODP Site 806) site used in the calibration study is $10.5 \mu\text{mol}$ (Wara et al., 2005), which is similar to Site U1451 ($0.24 \mu\text{mol}$). The dissolution corrected calibration that uses ΔCO_3^{2-} (Dekens et al., 2002) may be more accurate. The ΔCO_3^{2-} calibration corrects the Mg/Ca value using ΔCO_3^{2-} as a measure of dissolution at the deep water sediment/water interface (or as close as possible given data limitations) and simultaneously converts to Mg/Ca to SST (Dekens et al., 2002):

$$\text{Mg/Ca} = 0.31 \exp 0.084[\text{SST} + 0.048(\Delta\text{CO}_3^{2-})]$$

We calculated the modern ΔCO_3^{2-} at Site U1451, $\Delta\text{CO}_3^{2-} = 0.24 \mu\text{mol}$, using seawater temperature, salinity, and depth from the WOCE cruises. We used the modern ΔCO_3^{2-} value as an estimate for the ΔCO_3^{2-} at Site U1451 throughout the record which assumes that the carbonate ion concentration at this location has not changed significantly through the last 3.5 Ma. We know in the central equatorial Pacific that there have been variations in carbonate preservation since the early Pleistocene (Farrell & Prell, 1989; Broecker and Peng, 1982). However, we are assuming that the modern value of ΔCO_3^{2-} is appropriate for the ΔCO_3^{2-} downcore.

Finally, the Regenberg et al., 2006, provides an additional dissolution correction approach using core top samples from the Caribbean and the adjacent tropical Atlantic Ocean with a variety of water depths ranging from $\sim 900 - 4700 \text{ m}$. The calibration equation corrects Mg/Ca ratios for dissolution using species specific critical levels of

ΔCO_3^{2-} (Regenberg et al., 2006). The study was performed in a region where temperature-induced variability on Mg/Ca ratios were small, allowing for the isolation of the impact of calcite dissolution (Regenberg et al., 2006). This dissolution corrected Mg/Ca is then converted to SST using the Anand et al., 2003, SST calibration.

$$\text{Mg/Ca } (\Delta - \text{corrected}) = \text{Mg/Ca} + (\Delta - \Delta) / b$$

After converting Mg/Ca to SSTs, the dissolution corrected calibrations all yield similar SST estimates ($\sim 27^\circ\text{C}$ to $\sim 29^\circ\text{C}$ long term average SST; Figure 7), while the non-dissolution corrected calibration yields unrealistically low SST estimates ($\sim 25^\circ\text{C}$) (Table 2). The Anand et al., 2003 and Regenberg et al., 2006 approach yield a smaller SST variance (0.47°C) compared to the other dissolution corrections (0.92°C). The Dekens et al., 2002 ΔCO_3^{2-} corrected calibration was selected because core top samples most closely reflect modern SSTs (Table 2).

DISCUSSION

Generating paleoceanographic records in the Bengal Fan depositional environment is challenging, yet doing so provides an opportunity to further understand the role of the Indian Ocean during climate transitions. Our low-resolution SST record at Site U1451 shows no long-term trend in the southern Bay of Bengal since the Pliocene. SSTs at Site U1451 are stable and warm, mirroring what is seen in the western Equatorial

Pacific (Wara et al., 2005; Federov et al., 2013). These warm SSTs remain well within the range needed to create peak atmospheric convections that help support the AMS, which supports previous work that indicates the AMS has existed since the early Miocene.

Paleoceanographic reconstruction in sediment fan environments

The Bay of Bengal is a submarine fan (underwater alluvial fan) which is a challenging depositional environment to generate paleoceanographic records. Weathered terrestrial sediment from the Himalayan mountain range is transported by the Ganges-Brahmaputra-Meghna rivers (Subramanyam et al., 2008). The sediment laden rivers feed into the Bay of Bengal through the Ganges Delta, where a third of the sediment transported by the river system is deposited (Kuehl et al. 2007). The sediment is episodically transported from the continental shelf through a submarine canyon by turbidity currents which are responsible for the majority of sedimentation in the Bay of Bengal (Curry et al., 2003; Weber et al., 2003). Sedimentation resulting from these currents are referred to as turbidite deposits and are mostly comprised of sand. The foraminifera abundance within turbidite deposits are quite low (Frances-Lanord et al., 2015). However, core 1451A contains several hemipelagic sections comprised of a calcareous clay where the foraminifera abundance is much greater than that of the sandy turbidites.

Recent studies indicate that foraminifera within a levee deposit could have been transported from further north in the Bay of Bengal, where SST has a larger seasonal signal (Fritz-Endres et al., 2019; Figure 2). A levee is an area of high turbidity activity and the pelagic material from the overlying water column is mixed with the transported sediment (Frances-Lanord et al., 2015). This sediment could also have been reworked by further turbidity activity. The turbidite deposits at Site U1451 are likely from overspill or migration of an active channel (Curray et al., 2003).

Single foraminifera Mg/Ca and $\delta^{18}\text{O}$ analysis from core-tops at Sites U1454 and U1449 (both the same latitude as U1451) suggests that although foraminifera do record overlying water column conditions in hemipelagic sediments, caution must be taken when downcore lithologies indicate turbidite deposits (Fritz-Endres et al., 2019). The study showed that at Site U1454, which is located on the levee of the modern active channel, the foraminifera population represents a mixture of foraminifer transported from the northern Bay of Bengal (where SST and SSS have much larger seasonal variability) and from the overlying water column (Fritz-Endres & Dekens, 2019). In addition, the study demonstrated that foraminifera at Site U1449, which is 249 km away from Site U1454 and the modern channel/levee system, contains predominantly pelagic clay and foraminifera at this site reliably recorded sea surface conditions (Fritz-Endres & Dekens, 2019). This study demonstrates that foraminifera found in downcore hemipelagic calcareous clay sections not associated with a turbidite deposit reflect periods of time when pelagic sedimentation dominated, and reflect local conditions. We only sampled

foraminifera from the hemipelagic sections to avoid bias from transported foraminifera found in levee and turbidite sediments.

Foraminifera abundance was a critical limitation to the resolution of our temperature reconstruction. In addition to gaps from turbidite sections, some hemipelagic sections had too few foraminifera for geochemical analyses, creating further gaps. Gaps in the record range from 20ky to 500ky. Few long-term records exist in the Bay of Bengal due to these limitations. Our record therefore fills a data gap in the Indian Ocean that will further our understanding of tropical dynamics since the Pliocene. Although our new record is not able to resolve orbital scale climate variability, it does provide insight into long-term climate trends in the Indian Ocean.

SST records

Our Mg/Ca SST record from Site U1451 is a low resolution, long-term record that spans from the present through the late Pliocene (3.5 Ma). SST estimates range from ~26-31°C with a long-term average of 29.1°C. The resolution of our record is ~27ka in the hemipelagic sections of our core with periodic gaps of 20ky to 500ky.

An additional record from Site U1451 can be used to increase the resolution of our record. A high-resolution SST record of the Plio-Pleistocene transition (3.2 – 2.6 Ma) was constructed at Site U1451 from our laboratory (Cowan & Dekens, in progress). The study used the same paleothermometer and species of foraminifera and can therefore be

incorporated into our long-term record. The addition of the Plio-Pleistocene Mg/Ca SST record greatly increases our resolution during a critical climate transition where the global temperature was decreasing (Rohling et al., 2014).

Two records from Site U1452 (8°N, 87°E; ~3670m depth), ~70km west of Site U1451, can be used to further increase our SST record resolution. Both studies used the Mg/Ca ratios of *T. sacculifer* to reconstruct SST. Site U1452 experiences the same mean annual SST and seasonal SST range as Site U1451, indicating the two sites are experiencing the same sea surface conditions (Levitus, 1982). The proximity and similarity in ocean depth indicate that the foraminifera preservation is likely to be similar at the two sites. We therefore add these data to our record. The first SST record at Site U1452 is a high-resolution, ~2ky, record of SSTs over the last 180ky (Holmes & Dekens, 2017). The second is a high-resolution record that spans the Mid-Pleistocene Transition (Lagos & Dekens, 2018). The mean Mg/Ca values from Site 1451 and Site 1452 are almost indistinguishable, with a difference of ~0.02 mmol/mol. The distribution of both data sets appears normal and have a difference in standard deviation of ~0.02.

The age model for Sites U1451 is based predominantly on low-resolution magnetic reversals and biostratigraphy (France-Lanord et al., 2016). There are post-cruise efforts to improve the existing age model using a lithostratigraphy and sediment physical properties that vary on orbital timescales (Weber et al, 2018). For our purposes, the existing low-resolution age models constrain age well enough to perform long-term trend analysis. The Mg/Ca records from Site 1452 (Lagos & Dekens, 2018; Holmes & Dekens,

2017) were converted to SST using Dekens et al, 2002 ΔCO_3^{2-} calibration (Figure 8). The SST estimates from Sites U1451 and U1452 are consistent (Table 3; Figure 8).

Implications for the presence of AMS

The modern AMS is responsible for 1-4 meters of precipitation across east Asia and affects approximately one-third of the global population (Burbank et al, 2003). Differential heating of the Himalayan mountain range and the southern Indian Ocean creates an atmospheric pressure gradient. This pressure gradient generates a seasonal southwesterly wind (Schott et al., 2009; Zhisheng et al., 2015), which forces the summer monsoon current (Schott et al., 2009). The seasonal influx of warm SSTs, along with other atmospheric processes, create and sustain the AMS (Burbank et al, 2003). The modern monsoonal winds are upwelling favorable winds in the Arabian Sea & northern Bay of Bengal.

The AMS most likely existed in some form through the Pliocene and into the late-Miocene (Kroon et al., 1991; Zhisheng et al., 2001). Monsoonal winds force upwelling in the Arabian Sea. Therefore, variance in upwelling in the Arabian Sea would mean variance in the monsoonal wind patterns (Kroon et al., 1991). Kroon et al. (1991) were able to identify the onset or intensification of the AMS between 9-8 Ma by examining the increase in relative abundance of *Globigerina bulliodes* in the Arabian Sea. *G. bulliodes* is a planktonic species of foraminifera that prefers productive environments, and

therefore increases in abundance during periods of upwelling (Hemleben et al., 1989). The increase observed from 9-8 Ma in *G. bulliodes* abundance is an indication that greater upwelling had taken place meaning the onset or intensification of the AMS (Kroon et al., 1991).

A variety of studies from both oceanic and terrestrial paleoclimate data indicate that monsoons exist through the Pliocene and likely into the Miocene/Eocene (Kroon et al., 1991; Quan et al., 2012; Igarashi et al., 2018). The precipitation patterns indicated by fossil plant proxies displayed a strong seasonal signal, indicating the presence of a monsoonal system as early as the late Eocene (Quan et al., 2012). Plant assemblages from 37 locations across China indicate that mean annual precipitation was >735mm during the Eocene (Quan et al., 2012). A humid climate in East Asia would be associated with a monsoonal system (Igarashi et al., 2018). Pollen assemblages from the Japan Sea during the mid-Pliocene (~4.3 Ma) demonstrate a humid climate was present during this period (Igarashi et al., 2018).

Fully coupled global climate models indicate that the AMS could have existed as early as the Eocene, regardless of the Tibetan Plateau height (Huber & Goldner, 2012). The interaction between tectonics in East Asia (uplift of the Tibetan Plateau and Himalayas) and global climate change is the focal point of a host of different scientific research communities (Clemens et al., 2015; France-Lanord et al., 2016). Some studies indicate the uplift of the Tibetan Plateau and Himalayan mountain range could have strengthened the AMS or lead to the onset of the AMS (Zhisheng et al., 2001; Zheng et

al., 2004). Other studies using fully coupled global climate models have shown that the AMS would have existed regardless of the height of the Tibetan Plateau (Huber & Goldner, 2012; Ma et al., 2014). One such modeling study demonstrated the distribution of global monsoon precipitation existed as early as 45 Ma (Huber & Goldner, 2012). Using a combination of paleoclimate data as well as regional and global modeling know that the AMS has existed to some degree since the early Pliocene. Our data from the southern Bay of Bengal provides further evidence of the AMS existence during this period.

In the modern Bay of Bengal warm tropical waters are brought north into the Bay by the summer monsoon current. These waters travel past the location of Site U1451. These warm SSTs are responsible for increased atmospheric convection as well as latent heat, further fueling the AMS. Models indicate that modern SSTs need to be 26-30°C to create the atmospheric convection required to support the AMS (Tompkins, 2001). SSTs at our sites remain within this range throughout the past 3.5 Ma. Our SST record is further evidence that the AMS likely existed through the Pliocene.

Implications for the Indo-Pacific Warm Pool dynamics

The Indo-Pacific Warm Pool (IPWP) is a warm (~29°C year-round), stable pool of water that spans the western equatorial Pacific and the tropical Indian Ocean. The persistent warmth in the IPWP has a critical control on the regional and global climate.

The eastern equatorial Pacific is 4-5°C cooler, which creates a zonal SST gradient across the equatorial Pacific and drives the Walker Cell, an atmospheric convection cell across the equatorial Pacific. Fluctuations in the Walker Cell's strength are responsible for the El Niño Southern Oscillation (ENSO). El Niño events have a dramatic effect on regional climates, shifting precipitation patterns and warmth across the Pacific, and El Niño years are some of the warmest years on record with respect to the global average.

During the early Pliocene the climate of the tropical Pacific resembled that of an El Niño with a reduced zonal gradient and an increase in global average temperatures (Ford et al., 2015). The IPWP remained warm and stable while the eastern equatorial Pacific was 5-7°C warmer than modern values (Ford et al., 2015). Changes in SSTs patterns from the Pliocene to present establishes dramatically different regional climates, namely those in the eastern equatorial Pacific, and global climate (Ford et al., 2015).

We analyzed whether the southern Bay of Bengal, and more broadly the tropical Indian Ocean, exhibit characteristics seen in the tropical Pacific Ocean since the Pliocene. The closest record in proximity to Site U1451 is a Mg/Ca SST from ODP site 758 (5°N, 90°E in 2923m water depth), which has an average SST of 28.3°C since the early Pliocene (Dekens et al., 2008; Figure 9). The variance in SSTs at Site 758 ($\pm 1.3^\circ\text{C}$) is greater than that of Site U1451 ($\pm 0.93^\circ\text{C}$). Overall, the SSTs at Site U1451 track those of Site 758 quite well (Figure 9). Despite relatively stable SSTs through the last 5 Ma, there are brief periods of variability at Site 758. One of these periods occurs during the Plio-Pleistocene transition where it's believed that North Hemisphere glaciation began to

increase (Shackleton et al., 1988; Zachos et al., 2001). The SSTs at Site 758 cooled $\sim 2^{\circ}\text{C}$ during this time period. Additionally, it appears there is a small peak in SSTs during the Mid-Pleistocene Transition at Site 758. The SSTs at Site U1451/52 exhibited a similar range of temperature and variance to those of Site 758 during these key climate transitions.

ODP Site 806 (0°N , 159°E in 2520m water depth) is in the western equatorial Pacific (Table 3), and has a similarly stable SST pattern since the Pliocene (Wara et al., 2005; Figure 9). Similar to Site 758, there are brief periods of variability at Site 806 during climate transitions that are well matched by Site U1451/52 in mean temperature and variance. In stark contrast to the IPWP, the eastern equatorial Pacific exhibits a more pronounced cooling during climate transitions (Wara et al., 2005; Liu et al., 2004). These cooler mean temperatures are a result of upwelling and the more pronounced cooling during climate transitions could be the result of the intensification upwelling.

The SST pattern in the Bay of Bengal through the last 3.5 Ma closely tracks other records in the IPWP. This tells us that the IPWP stretched as far north as Site U1451 & U1452 (8°N) through the Pliocene. These results support the previous observations of a stable IPWP through the Pliocene even as the Eastern Equatorial Pacific and global temperatures cool (Fedorov et al., 2013; Rohling et al., 2014). These warm SSTs would have sustained atmospheric convection and provide the fuel for monsoonal events such as the seasonal AMS. It should be noted that Site U1451 & U1452 are too far south in the Bay of Bengal to record any direct indications of monsoon activity. Future work in

collaboration with records from Expedition 353 with sites in the northern Bay of Bengal would provide a greater understanding of the AMS and its evolution since the Pliocene.

CONCLUSIONS

In this study we reconstructed oceanographic conditions at site U1451 through the Pliocene despite limitations related to a sediment fan environment. These conditions did, however, limited our data to a low-resolution record that include gaps of 20-500ky. The *T. sacculifer* Mg/Ca successfully and reliably recorded SST (Figures 7). A calibration that includes a dissolution correction is clearly needed for the southern Bay of Bengal (Table 2). There is no long-term SST trend at Site U1451/52 through the last 3 Ma; SST remains relatively stable with an average SST of $\sim 29^{\circ}\text{C}$ (Figure 8). This is consistent with other SST reconstructions from the IPWP (Figure 9). This indicates that the IPWP spread as far north as Site 1451/52 (8°N) through the Pliocene and demonstrates agreement with previous studies that show a warm and stable IPWP through the Pliocene. SSTs remain within the range ($26\text{-}30^{\circ}\text{C}$) required to support the modern AMS.

FUTURE WORK

More Mg/Ca data are needed to complete the SST record into the early Pliocene (to 5 Ma); 65 samples from the early Pliocene remain to be analyzed. However, gaps will remain in the record due to lithology and preservation. We hypothesize the consistency with the IPWP continues through the early Pliocene. Additionally, we plan to use $\delta^{18}\text{O}$ analysis of *T. sacculifer* to provide a record of the evolution of $\delta^{18}\text{O}$ of seawater through this time period and provide insight into the role of AMS or the IPWP air-sea interactions through the Pliocene. Future work will include the reconstruction of the subsurface conditions at Site U1451 using *G. tumida* Mg/Ca. Mg/Ca analysis of *G. tumida* will reconstruct temperatures at ~100m water depth at Site U1451 through the Pliocene, providing an opportunity to compare the structure of the thermocline in the Bay of Bengal to those in the IPWP that demonstrate a shoaling since the early Pliocene. Additionally, the implications of stable SSTs at Site U1451/52 will need to be examined in relation to the results of IODP Expedition 353 whose intentions were to study the evolution of the AMS in the northern Bay of Bengal.

REFERENCES

- Anand, P., H. Elderfield, and M. H. Conte (2003), Calibration of Mg/Ca thermometry in planktonic foraminifera from a sediment trap time series. *Paleoceanography*, 18, 1050.
- Bé, A. W. H., Spero, H. J., & Anderson, O. R. (1982). Effects of symbiont elimination and reinfection on the life processes of the planktonic foraminifer *Globigerinoides sacculifer*. *Marine Biology*, 70(1), 73–86.
- Boyle, E.A. (1981). Cadmium, Zinc, Copper, and Barium in foraminifera test. *Earth & Planetary Science Letters*, 53(1981), 11-35.
- Boyle, E.A. (1983). Manganese carbonate overgrowths on foraminifera tests. *Geochimica et Cosmochimica Acta*, 47, 1815-1819.
- Boyle, E. A., & Keigwin, L. D. (1985). Comparison of Atlantic and Pacific paleochemical records for the last 215,000 years: changes in deep ocean circulation and chemical inventories. *Earth and Planetary Science Letters*, 76(1–2), 135–150.
- Brierley, C., Burls, N., Ravelo, C., & Fedorov, A.. (2015). Pliocene warmth and gradients. *Nature Geoscience*, 8(6), 419-420.
- Brierley, C., & Fedorov, A., (2010). Relative importance of meridional and zonal sea surface temperature gradients for the onset of the ice ages and Pliocene-Pleistocene climate evolution. *Paleoceanography*, 25.
- Broecker, W. S., & Peng, T., (1982). Tracers in the sea. *Lamont-Doherty Geological Observatory, Columbia University, Palisades, New York*.
- Brummer, G. J. A., Hemleben, C., & Spindler, M. (1986). Planktonic foraminiferal ontogeny and new perspectives for micropalaeontology. *Nature*, 319(6048), 50–52.
- Burbank, D. W., Blythe, A. E, Putkonen, J, Pratt-Sitaula, B, Gabet, E, Oskin, M, Ojha, T. P., (2003). Decoupling of Erosion and Precipitation in the Himalayas. *Nature*, 426(6967), 652–655.

- Clemens, S. C., Kuhnt, W., & Levay, L. J. (2015). Expedition 353 Preliminary Report, (November 2014).
- Cowan, K., & Dekens, P., (2020). Sea Surface Conditions in the Bay of Bengal Through the Pliocene-Pleistocene Cooling. (Unpublished master's thesis). San Francisco State University, California, U.S. Unpublished Raw Data.
- Curray, J. R., Emmel, F. J. & Moore, D. G., (2003). The Bengal Fan: morphology, geometry, stratigraphy, history and processes. *Mar. Petrol. Geol.* 19, 1191–1223.
- Deer, W. A., R. A. Howie, and J. Zussman, (1992). An Introduction to the Rock Forming Minerals, 2 ed., Addison-Wesley-Longman, Reading, Mass.
- Dekens, P., D. Lea, D. Pak, and H. Spero (2002), Core top calibration of Mg/Ca in tropical foraminifera: Refining paleotemperature estimation, *Geochem. Geophys. Geosyst.* 3(4).
- Dekens, P., Ravelo, A., & McCarthy, M. (2007). Warm upwelling regions in the Pliocene warm period. *Paleoceanography*, 22(3).
- Dekens, P., Ravelo, C., McCarthy, M., & Edwards, C., (2008). A 5 million year comparison of Mg/Ca and alkenone paleothermometers. *Geochemistry Geophysics Geosystems*, 9(10), Q10001.
- Delaney, M.L., Be, A., & Boyle E.A., (1985). LI, SR, MG, AND NA in foraminiferal calcite shells from laboratory culture, sediment traps, and sediment cores. *Geochimica et Cosmochimica Acta*, 49(6), 1327-1341.
- Eggins, S., De Deckker, P., Marshall, J. (2003). Mg/Ca variation in planktonic foraminifera tests: implications for reconstructing palaeo-seawater temperature and habitat migration. *Earth and Planetary Science Letters* (212, 3-4) 291-306.
- Elderfield, H., & Ganssen, G. (2000). Past temperature and $\delta^{18}\text{O}$ of surface ocean waters inferred from foraminiferal Mg/Ca ratios. *Nature*, 405(6785), 442.
- Elderfield, H., Yu, J., Anand, P., Kiefer, T., & Nyland, B. (2006). Calibrations for benthic foraminiferal Mg / Ca paleothermometry and the carbonate ion hypothesis. *Earth and Planetary Science Letters*, 250, 633–649.
- Farmer, C., Kaplan, A., B. de Menocal, P., Lynch-Stieglitz, J., (2007). Corroborating ecological depth preferences of planktonic foraminifera in the tropical Atlantic with the stable oxygen isotope ratios of core top specimens. *Paleoceanography*, 22, PA3205.

- Farrell, J., & Prell, W., (1982). Climate change and CaCO₃ preservation: an 800,000 year bathymetric reconstruction from the central equatorial Pacific ocean. *Paleoceanography*, 4(4), 447-466.
- Fedorov, A. V., C. M. Brierley, K. T. Lawrence, Z. Liu, P. S. Dekens, and A. C. Ravelo, (2013). Patterns and mechanisms of early Pliocene warmth. *Nature*, 496, 43–49.
- Feely, R., Sabine, C., Lee, K., & Berelson, W. (2004). Impact of Anthropogenic CO₂ on the CaCO₃ System in the Oceans. *Science*, 305(5682), 362-6.
- Ford, Heather L, Ravelo, A. Christina, & Hovan, Steven. (2012). A deep Eastern Equatorial Pacific thermocline during the early Pliocene warm period. *Earth and Planetary Science Letters*, 355-356, 152-161.
- Ford, H.L., Ravelo, A.C., Dekens, P.S., Lariviere, J.P., Wara, W.M., (2015). The evolution of the equatorial thermocline and the early Pliocene El Padre mean state. *Geophys. Res. Lett.* 42, 4878–4887.
- France-Lanord, C., Spiess, V., Klaus, A., Adhikari, R.R., Adhikari, S.K., Bahk, J.-J., Baxter, A.T., Cruz, J.W., Das, S.K., Dekens, P., Duleba, W., Fox, L.R., Galy, A., Galy, V., Ge, J., Gleason, J.D., Gyawali, B.R., Huyghe, P., Jia, G., Lantzsch, H., Manoj, M.C., Martos Martin, Y., Meynadier, L., Najman, Y.M.R., Nakajima, A., Ponton, C., Reilly, B.T., Rogers, K.G., Savian, J.F., Schwenk, T., Selkin, P.A., Weber, M.E., Williams, T., and Yoshida, K., 2016b. Site U1454. In France-Lanord, C., Spiess, V., Klaus, A., Schwenk, T., and the Expedition 354 Scientists, *Bengal Fan*. Proceedings of the International Ocean Discovery Program, 354: College Station, TX (International Ocean Discovery Program).
- Fritz-Endres, T., Dekens, P., Fehrenbacher, J., Spero H., Stine, A., (2019). Application of individual foraminifera Mg/Ca and d¹⁸O analyses for paleoceanographic reconstructions in active depositional environments. *Paleoceanography*.
- Galy, V., France-Lanord, C., Beyssac, O., Faure, P., Kudrass, H., and Palhol, F., (2007). Efficient organic carbon burial in the Bengal Fan sustained by the Himalayan erosional system. *Nature*, 450(7168):407–410.
- Gordon, A., Shroyer, E., Mahadevan, A., Sengupta, D., & Freilich, M. (2016). Bay of Bengal 2013 Northeast Monsoon Upper-Ocean Circulation. *Oceanography*, 29(2), 82-91.

- Gray, Weldeab, Lea, Rosenthal, Gruber, Donner, & Fischer, (2018). The effects of temperature, salinity, and the carbonate system on Mg/Ca in Globigerinoides ruber (white): A global sediment trap calibration. *Earth and Planetary Science Letters*, 482, 607-620.
- Hawkins E., Ortega P., Suckling E., Schurer A., Hegerl G., Jones, P., Oldenborgh, G., (2017). Estimating changes in global temperature since the preindustrial period. *Bulletin of the American Meteorological Society*, 98(9), 1841-1856.
- Herbert, T. D, Peterson, L. C, Lawrence, K. T, & Liu, Z. (2010). Tropical Ocean Temperatures Over the Past 3.5 Million Years. *Science (American Association for the Advancement of Science)*, 328(5985), 1530-1534.
- Hemleben, Spindler, Anderson, Spindler, Michael, & Anderson, O. Roger. (1989). Modern planktonic foraminifera. New York: Springer-Verlag.
- Holmes, B., & Dekens, P. S. (2017). Ocean Conditions in the Southern Bay of Bengal during the Last Glacial Cycle. Senior Thesis. San Francisco State University. Unpublished Raw Data.
- Huber, Matthew, & Goldner, Aaron. (2012). Eocene monsoons. *Journal of Asian Earth Sciences*, 44, 3-23.
- Igarashi, Y., Irino, T., Sawada, K., Song, L., & Furota, S., (2018). Fluctuations in the East Asian monsoon recorded by pollen assemblages in sediments from the Japan Sea off the southwestern coast of Hokkaido, Japan, from 4.3 Ma to the present. *Global and Planetary Change*, 163, 1-9.
- IPCC, 2014: Annex II: Glossary [Mach, K.J., S. Planton and C. von Stechow (eds.)]. In: Climate Change 2014: Synthesis Report. Contribution of Working Groups I, II and III to the Fifth Assessment Report of the Intergovernmental Panel on Climate Change [Core Writing Team, R.K. Pachauri and L.A. Meyer (eds.)]. IPCC, Geneva, Switzerland, pp. 117-130.
- Karas, Cyrus, Tiedemann, Ralf, Mohan, Kuppusamy, , Bickert, Torsten, Gupta, Anil K, & Nürnberg, Dirk. (2009). Mid-Pliocene climate change amplified by a switch in Indonesian subsurface throughflow. *Nature Geoscience*, 2(6), 434-438.
- Karas, C., Nuernberg, D., Tiedemann, R., Garbe-Schoenberg, D., Nürnberg, D., & Garbe-Schönberg, Di., (2011). Pliocene Indonesian Throughflow and Leeuwin Current dynamics: Implications for Indian Ocean polar heat flux. *Paleoceanography*, 26(2).

- Kennett, J., & Srinivasan, M. (1983). Neogene planktonic foraminifera: A phylogenetic atlas. Stroudsburg, Pa.: New York, NY: Hutchinson Ross; Distributed by worldwide by Van Nostrand Reinhold.
- Kudrass, H.R., Hofmann, A., Doose, H., Emeis, K., Erlenkeuser, H. (2001). Modulation and amplification of climatic changes in the Northern Hemisphere by the Indian summer monsoon during the past 80 k.y. *Geology* (29,1) 63-66.
- Kroon, S., Steens, T., Troelstra, S.R., (1991). Onset of monsoonal related upwelling in the western Arabian Sea as revealed by planktonic foraminifers. Proceedings of the Ocean Drilling Program. Scientific Results 117, 257–263.
- Kuehl, S.A., Levy, B.M., Moore, W.S., Allison, M.A., (1997). Sub-aqueous delta of the Ganges–Brahmaputra river system. *Mar. Geol.* 144, 81–96.
- Lagos, L., & Dekens, P., (2018). Oceanographic conditions in the southern Bay of Bengal from ~0.8 – 1.3Ma. (Unpublished master's thesis). San Francisco State University, California, U.S. Unpublished Raw Data.
- Levitus, S. (1982). Climatological atlas of the world ocean. *US Government Printing Office, Washington DC, NOAA Prof(13)*.
- Li, X., Zhang, R., Zhang, Z., & Yan, Q. (2018). Do climate simulations support the existence of East Asian monsoon climate in the Late Eocene? *Palaeogeography, Palaeoclimatology, Palaeoecology*, 509, 47-57.
- Lisiecki, L. E., & Raymo, M. E. (2005). A Pliocene-Pleistocene stack of 57 globally distributed benthic $\delta^{18}\text{O}$ records. *Paleoceanography*, 20(1), 1–17.
- Liu, Z., & Herbert, T. (2004). High-latitude influence on the eastern equatorial Pacific climate in the early Pleistocene epoch. *Nature (London)*, 427(6976), 720-723.
- Ma, D., Boos, W., & Kuang, Z. (2014). Effects of Orography and Surface Heat Fluxes on the South Asian Summer Monsoon. *Journal of Climate*, 27(17), 6647-6659.
- Martin, P. A., & Lea, D. W. (2002). A simple evaluation of cleaning procedures on fossil benthic foraminiferal Mg/Ca. *Geochemistry, Geophysics, Geosystems*, 3(10), 1–8.
- Medina-Elizalde, M., and D. W. Lea (2005), The mid-Pleistocene transition in the tropical Pacific. *Science*, 310, 1009– 1012.

- Molnar, P., Boos, W. R., & Battisti, D. S. (2010). Orographic Controls on Climate and Paleoclimate of Asia: Thermal and Mechanical Roles for the Tibetan Plateau. *Annu Rev Earth Planet Sci*, 38(1), 77–102.
- Poole, C., & Wade, B. (2019). Systematic taxonomy of the *Trilobatus sacculifer* plexus and descendant *Globigerinoidesella fistulosa* (planktonic foraminifera). *Journal of Systematic Palaeontology*, 17(23), 1989-2030.
- Quan, Cheng, Liu, Yu-Sheng, & Utescher, Torsten. (2012). Eocene monsoon prevalence over China: A paleobotanical perspective. *Palaeogeography, Palaeoclimatology, Palaeoecology*, 365-366, 302-311.
- Quinn, W.H., Neal, V., Demayolo, S., (1987). El Nino occurrences over the past 4-1/2 centuries. *Journal of Geo Phy Res- Oceans*, 92(C13), 14449-14461.
- Ravelo, A. C., & Fairbanks, R. G. (1992). Oxygen isotopic composition of multiple species of planktonic foraminifera: Recorders of the modern photic zone temperature gradient. *Paleoceanography*, 7(6), 815–831
- Ravelo, C., Wara, M., Andreasen, D., Lyle, M., & Olivarez Lyle, A. (2004). Regional climate shifts caused by gradual global cooling in the Pliocene epoch. *Nature*, 429(6989), 263-267.
- Ravelo, C., Hillaire-Marcel, C., (2007). The use of oxygen and carbon isotopes of foraminifera in paleoceanography. *Developments in Marine Geology*. 1: 735-764.
- Raymo, M.E., and Ruddiman, W.F. (1992). Tectonic forcing of late Cenozoic climate. *Nature* 359(6391):117–122.
- Raymo, M.E, Grant, B, Horowitz, M, & Rau, G.H. (1996). Mid-Pliocene warmth: Stronger greenhouse and stronger conveyor. *Marine Micropaleontology*, 27(1), 313-326.
- Regenberg, M., Nürnberg, D., Steph, S., Groeneveld, J., Garbe-Schönberg, D., Tiedemann, R., & Dullo. W., (2006). Assessing the effect of dissolution on planktonic foraminiferal Mg/Ca ratios: Evidence from Caribbean core tops. *Geochemistry Geophysics Geosystems*, 7(7), Q07P15.
- Robinson, M., Dowsett, H. J., Chandler, M. A. (2008). Pliocene role in assessing future climate impacts. *Eos*. 89 (49): 501–502.

- Rohling, E., Foster, G., Grant, K., Marino, G., Roberts, A., Tamisiea, M., & Williams, F. (2014). Sea-level and deep-sea-temperature variability over the past 5.3 million years. *Nature*, 508(7497), 477-482.
- Schott, F. A., Xie, S.-P., & McCreary Jr, J. P. (2009). Indian Ocean Circulation and Climate Variability. *Reviews of Geophysics*, 47, 1–46.
- Shackleton, N. J., Berger, A., & Peltier, W. R. (1990). An alternative astronomical calibration of the lower Pleistocene timescale based on ODP Site 677. *Transactions of the Royal Society of Edinburgh, Earth Science*(81), 251–261.
- Spero, H. , & Lea, D. (1996). Experimental determination of stable isotope variability in *globigerina bulloides*: Implications for paleoceanographic reconstructions. *Marine Micropaleontology*, 28(3-4), 231-246.
- Stap, L.B., De Boer, B., Ziegler, M., Bintanja, R., Lourens, L.J., & Van de Wal, R., (2016). CO₂ over the past 5 million years: Continuous simulation and new $\delta^{11}\text{B}$ -based proxy data. *Earth and Planetary Science Letters*, 439, 1-10.
- Tompkins, A. (2001). On the relationship between tropical convection and sea surface temperature. *Journal of Climate*, 14, 633–637.
- Vail, P.R., Audemard, F., Bowman, S.A., Eisner, P.N., Perez-Cruz, G., (1991). The stratigraphic signatures of tectonics, eustasy and sedimentation – An overview. In: Einsele, G., Ricken, W., Seilacher, A. (Eds.), *Cyclic stratigraphy II*. Springer-Verlag, New York, pp. 617– 659
- Wang, Q., Spicer, R., Yang, J., Wang, Y., & Li, C.. (2013). The Eocene climate of China, the early elevation of the Tibetan Plateau and the onset of the Asian Monsoon. *Global Change Biology*, 19(12), 3709-3728.
- Wara, M. W., Ravelo, A. C., & Delaney, M. L. (2005). Climate change: Permanent El Niño-like conditions during the Pliocene warm period. *Science*, 309(5735), 758–761.
- Wasson, R.J., (2003). A sediment budget for the Ganga-Brahmaputra catchment. *Current Science*, 84(8): 1041-1047.

- Weber, M., Wiedicke-Hombach, M., Kudrass, H., & Erlenkeuser, H., (2003). Bengal fan sediment transport activity and response to climate forcing inferred from sediment physical properties. *Sedimentary Geology*, 155(3), 361-381.
- Weber, M., & Reilly, B., (2018). Hemipelagic and turbiditic deposits constrain lower Bengal Fan depositional history through Pleistocene climate, monsoon, and sea level transitions. *Quaternary Science Reviews*. 199. 159-173.
- White, S. M., & Ravelo, A. C., (2020). Dampened El Niño in the early Pliocene warm period. *Geophysical Research Letters*, 47.
- Zachos, J. (2001). Trends, Rhythms, and Aberrations in Global Climate 65 Ma to Present. *Science (American Association for the Advancement of Science)*, 292(5517), 686-693.
- Zheng, H. (2004). Late Miocene and mid-Pliocene enhancement of the East Asian monsoon as viewed from the land and sea. *Global and Planetary Change*, 41(3-4), 147-155.
- Zhisheng, A., Kutzbach, J.E., Prell, W.L., Porter, S.C., (2001). Evolution of Asian monsoons and phased uplift of the Himalaya–Tibetan plateau since Late Miocene times. *Nature* 411, 62- 66.

APPENDICES

Appendix 1 – *T. sacculifer* taxonomic identification

T. sacculifer were identified by its three near spherical chambers with a single, primary aperture (Kennett & Srinivasan, 1983). *T. sacculifer* wall texture is coarsely cancellate (sugary, or honeycomb in appearance) (Kennett & Srinivasan, 1983). *T. sacculifer* is distinguished from similarly taxonomic foraminifera (e.g. *Trilobatus immaturus* and *Trilobatus quadrilobatus*) by its fourth flattened, sac-like chamber (Poole & Wade, 2019). However, juvenile *T. sacculifer* were preferentially selected because during the adult stage *T. sacculifer* migrate deeper, grow the fourth characteristic sac-like chamber as well as gametogenic calcite, inhibiting the shells use as a geochemical proxy (Bé et al., 1982; Brummer et al., 1986). We used the *T. sacculifer*'s distinctive lip bordering the primary aperture to distinguish from similar foraminifera (Poole & Wade, 2019).

Appendix 2– Cleaning Procedures

Each sample received three rinses with ultra-pure (Milli-Q) deionized water, two rinses with methanol, followed by three additional rinses with ultra-pure (Milli-Q) deionized water. Samples receive 30 seconds of ultra-sonication in-between each rinse. It's important to be particularly rigorous during the initial rinses as silicate removal has the greatest influence on sample Mg/Ca ratio during the cleaning process (Barker et al., 2003). These clays can contain 1-10% Mg by weight. (Deer et al., 1992).

During the reductive step, designed to remove manganese oxides, 100 μ l of a solution of 10ml ammonium citrate, 10ml ammonium hydroxide, and 1ml 85% anhydrous aqueous hydrazine was added to each sample. Outgassing requires the caps to each sample's vial be securely closed. A flat, acrylic plate is fastened atop the caps of the samples to prevent opening of the vials during a 30-minute hot water bath (180-200°F). Samples were inverted and received five second ultra-sonication at two-minute intervals during the 30-minute hot water bath. The reaction was stopped with a quick rinse of ultra-pure deionized water, followed by three ultra-pure water rinses with 30 second ultra-sonication between each before proceeding to the oxidation step.

Organic material was removed during the oxidation step by adding 250 μ l of a solution of 50 μ l 30% hydrogen peroxide and 30ml of 0.1N sodium hydroxide to each sample (Barker et al., 2003). The samples were then placed in a 10-minute hot water bath with a 5 second ultra-sonication after 5 and 10 minutes. The reaction was stopped, and the solution removed with a quick rinse of ultra-pure deionized water, followed by two ultra-pure water rinses with no ultra-sonication between each. The samples were then placed in a 5-minute hot water bath with a 5 second ultra-sonication both before and after the bath. Then samples underwent another rinse with ultra-pure water including a 30 second ultra-sonication.

Samples were covered with ultra-pure water and transferred from 0.5 mL vials to 1.5 mL vials where they received a weak acid leach to remove any reabsorb authigenic contaminants (Martin & Lea, 2002). Ultra-pure water was added to each sample and the

acid was siphoned away, followed by two additional rinses of ultra-pure water to remove any remaining acid. The cleaned samples were run on an Inductively Coupled Plasma Optical Emission Spectrometer (ICP-OES) at the at the UC Santa Cruz Marine Analytical Lab.

Appendix 3 – Mn/Ca

Included in my sampling were 28 replicates that were cleaned at a separate facility, University of California Santa Cruz Marine Analytical Laboratory. The average difference in Mg/Ca values between replicates is 0.024 mmol/mol. The average difference in Mn/Ca values between replicates is 0.013 mmol/mol. The Shapiro Wilks test showed that the Mg/Ca and the Mn/Ca of the replicates were all normally distributed with all p values greater than my alpha level of 0.5. A parametric matched pairs test and a nonparametric Wilcoxon sign ranked test of both Mg/Ca and Mn/Ca resulted in significantly higher than alpha (0.05) p values indicating there is no statistical difference between the replicates. Density ellipse were used on pairs of data to determine their correlation. Mn/Ca values demonstrated a statistically significant (p-value = <0.0001; alpha level = 0.05) correlation of 0.83. However, the correlation between paired Mg/Ca values was low ($r = 0.33$) and not statistically significant (p-value = 0.089).

TABLES

Pliocene Age Model

Site	Depth CSF-A (m)	Age (Ma)	Sedimentation rate (cm/ka)	Stratigraphic Tie Point
U1451A	72.24	0.781	9.25	Bruhnes / Matuyama
U1451A	80.35	0.998	3.74	Jaramillo
U1451A	81.78	1.072	1.93	Matuyama
U1451A	83.1	1.173	1.31	Cobb Mountain
U1451A	83.44	1.185	2.83	Matuyama
U1451A	130.06	2.58	3.34	
U1451A	143	3.596	1.27	Gilbert
U1451A	152.99	4.493	1.11	Nunivak
U1451A	155.8	4.631	2.04	Gilbert
U1451A	161.1	4.896	2.00	Gilbert
U1451A	163.07	4.997	1.95	Thvera
Average Sedimentation rate			2.80	

Table 1

Mg/Ca Calibrated SSTs at Site U1451

Calibration Method	Range (°C)	Mean (°C)
Anand et al., 2003	21.8 – 26.6	24.4
Dekens et al., 2002 (WD)	25.4 – 30.2	27.9
Dekens et al., 2002 (ΔCO_3^{2-})	25.8 – 30.9	29.1
Regenberg et al., 2006	25.5 – 29.1	27.1
Modern SSTs at Site U1451A	27.6 – 30.0	28.5

Table 2

Pliocene – Present Tropical SSTs

Site	Location	Range (°C)	Mean (°C)
IODP U1451	S. Bay of Bengal	25.8 – 30.9	29.1
IODP U1452	S. Bay of Bengal	24.9 – 31.2	28.6
ODP 806	W. Equatorial Pacific	25.0 – 32.9	29.2
ODP 758	Equatorial Indian	23.6 – 31.1	28.1
ODP 847	E. Equatorial Pacific	21.3 – 29.9	26.6

Table 3

FIGURES

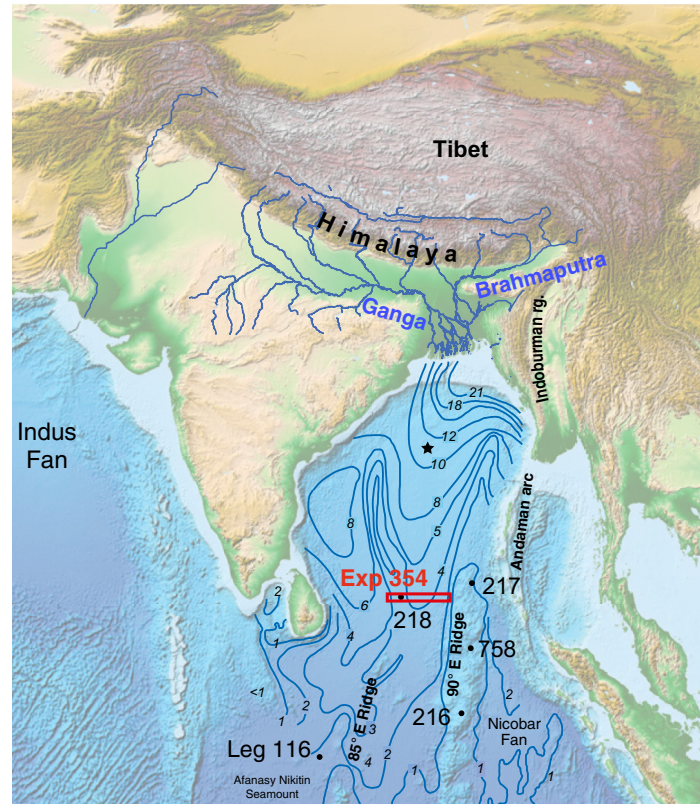


Figure 1 A map highlighting IODP Expedition 354 transect (red box) along 8°N where drilled 7 sites in the southern Bay of Bengal (France-Lanord et al., 2016). Blue contour lines represent fan thickness (km).

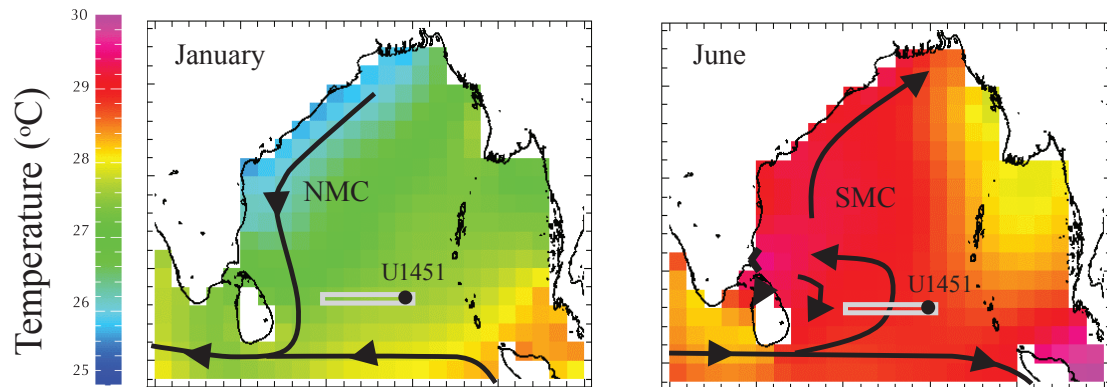


Figure 2 Modern SSTs in the Bay of Bengal during the months of January and June (Levitus, 1982). Black arrows highlight the seasonal currents in the Bay of Bengal, the Northern Monsoon Current (NMC) and Southern Monsoon Current (SMC) (Schott et al., 2009). Expedition 354 is located in the path of the SMC, which transports warm water from the tropics to the northern Bay of Bengal during summer (Schott et al., 2009).

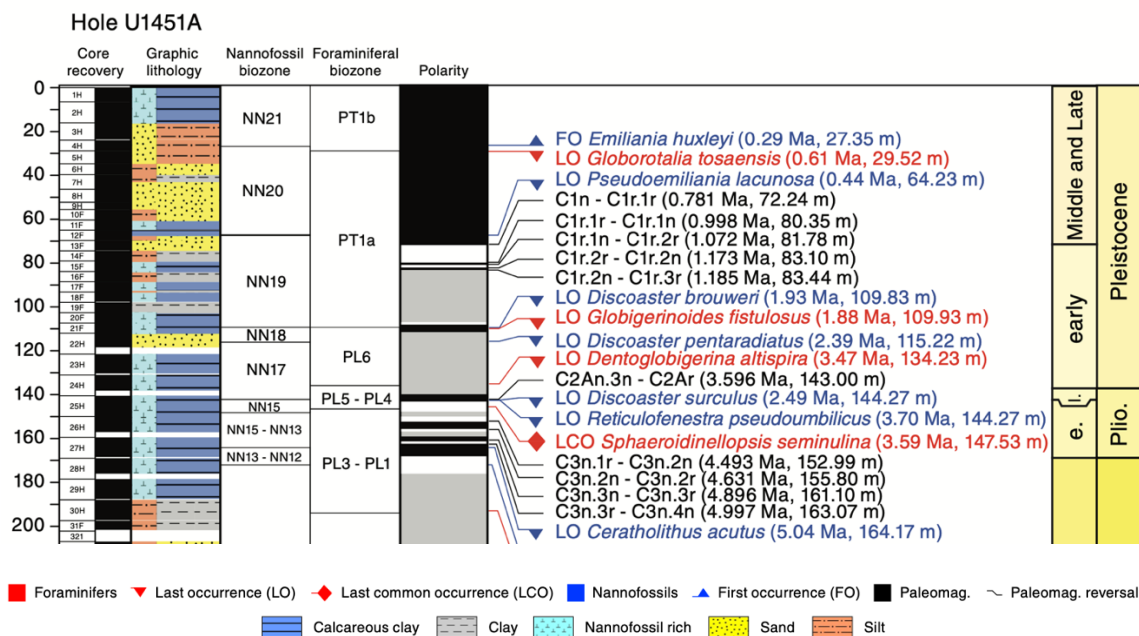


Figure 3 Hole U1451A chronostratigraphic and biostratigraphic markers within the top 200 m of the core. Biomarkers were calculated as midpoints. The boundaries of the paleomagnetic reversals are the lower depth of the reversal. (Frances-Lanord et al., 2016)

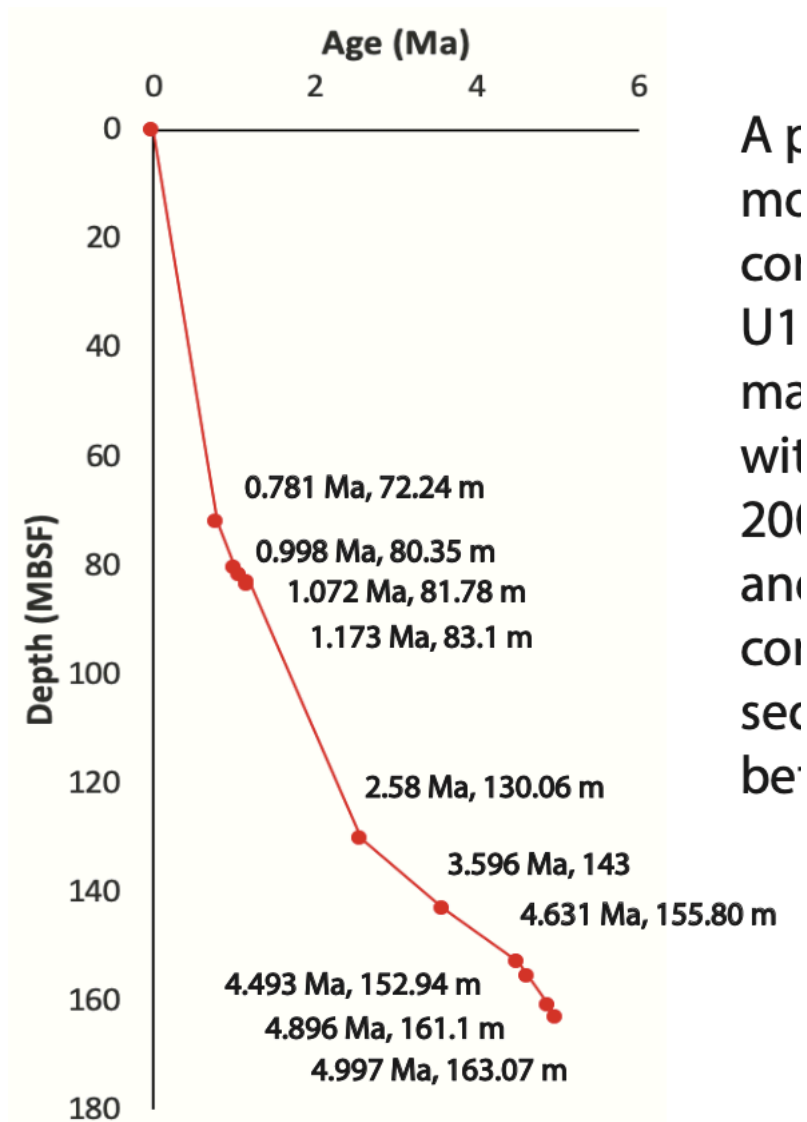


Figure 4 Site U1451 age model where the depth is converted to age using magnetic reversals as tie points and sedimentation interpolated between points.

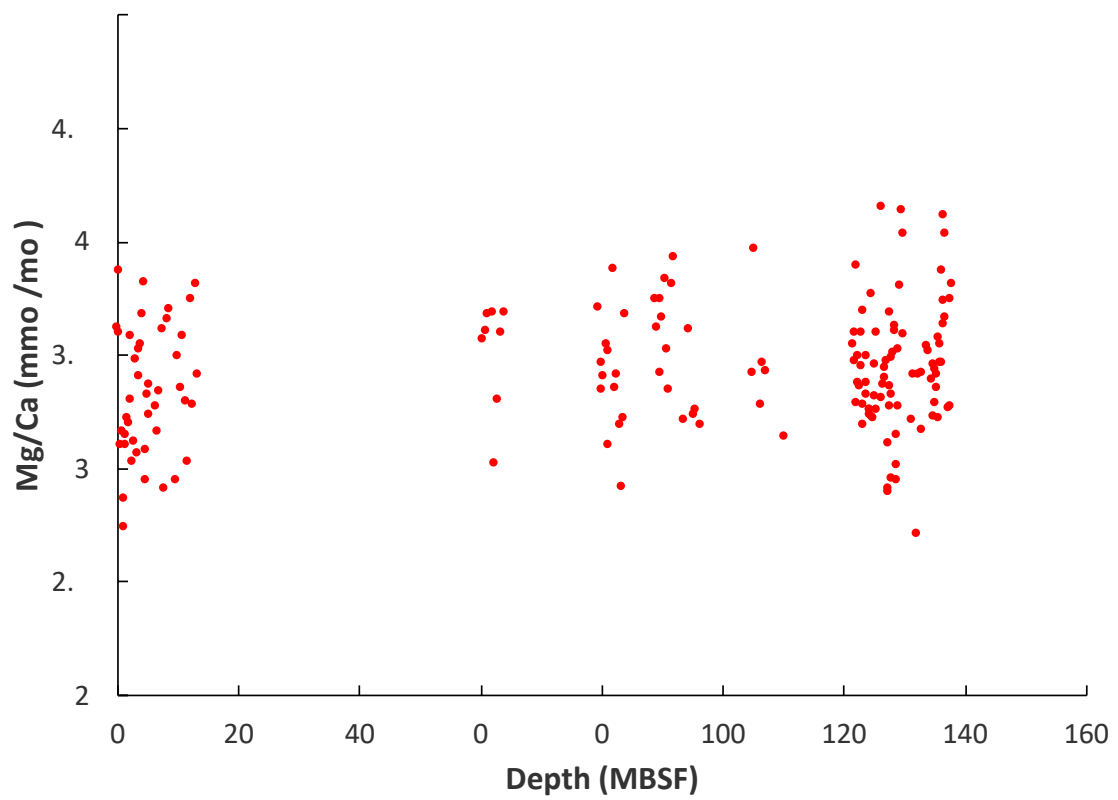


Figure 5 *T. sacculifer* Mg/Ca at Site U1451. Mg/Ca values range from 2.7 – 4.1 mmol/mol.

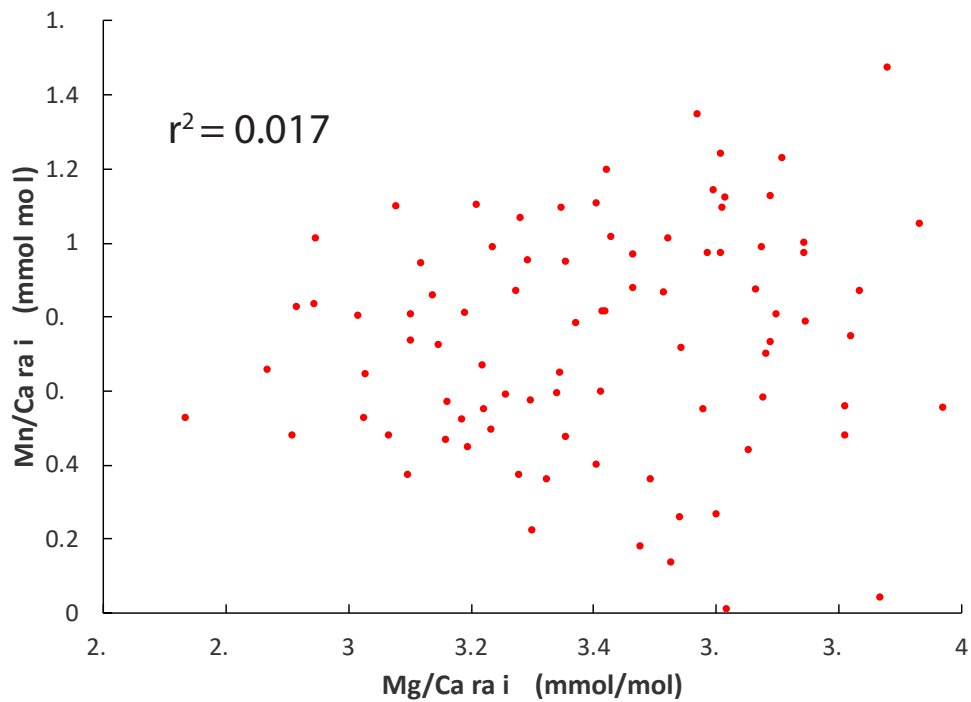


Figure 6 Scatter plot of *T. sacculifer* Mn/Ca & Mg/Ca ratios to determine if there is any correlation. A correlation between Mn/Ca & Mg/Ca values would indicate biased Mg/Ca due to insufficient cleaning or the existence of a Mn-overcoat.

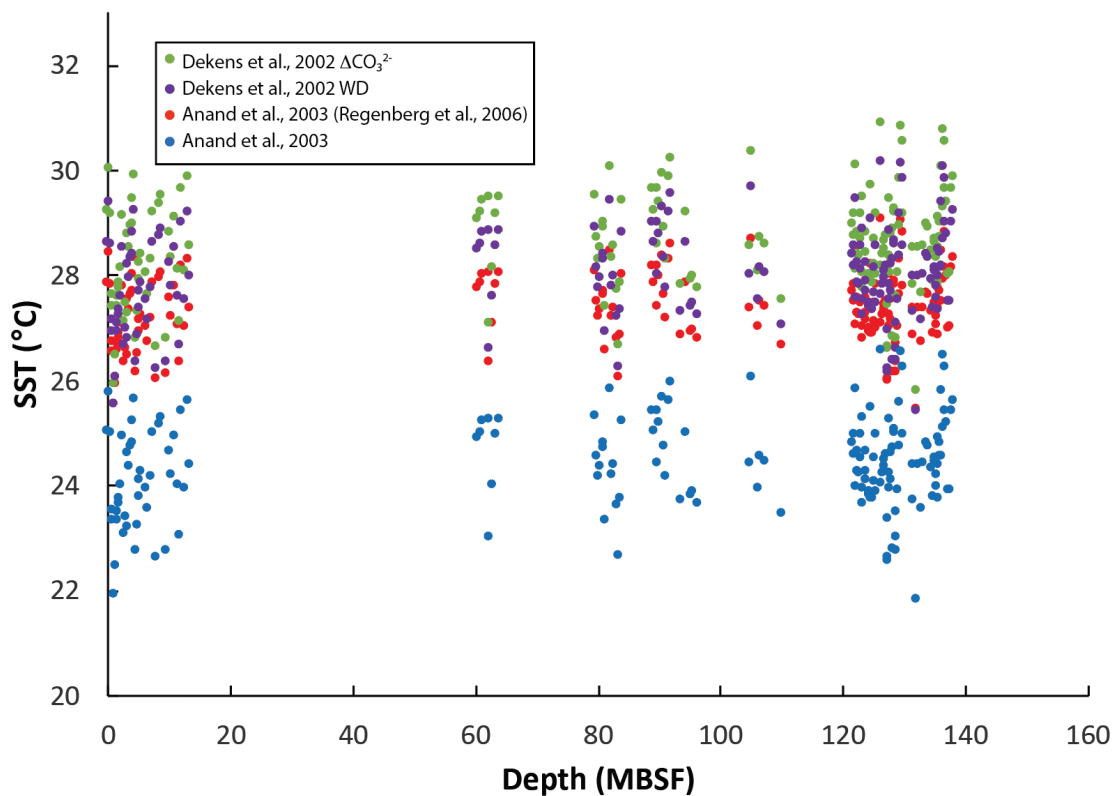


Figure 7 A comparison four SST calibration equation. One calibration that is created using cultures studies (light green; Anand et al., 2003) and three calibrations based on core top studies that include a dissolution correction (Dekens et al., 2002; Regenberg et al., 2006) used to generate the Site 1451 SST record.

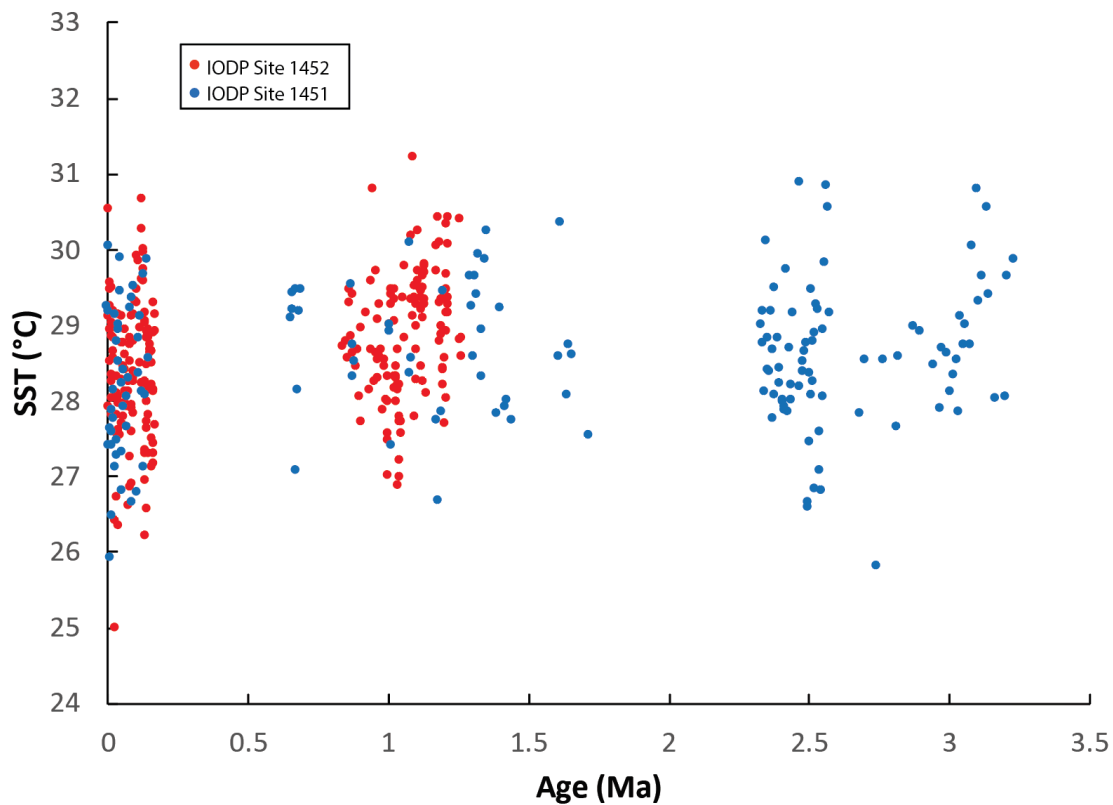


Figure 8 SSTs at Site U1451& U1452 using the Dekens et al., 2002, ΔCO_3 calibration. We include data from IOPD Site U1452, which is only ~70km west and at a similar depth to that of Site U1451 and therefore records the same sea surface conditions and dissolution effect.

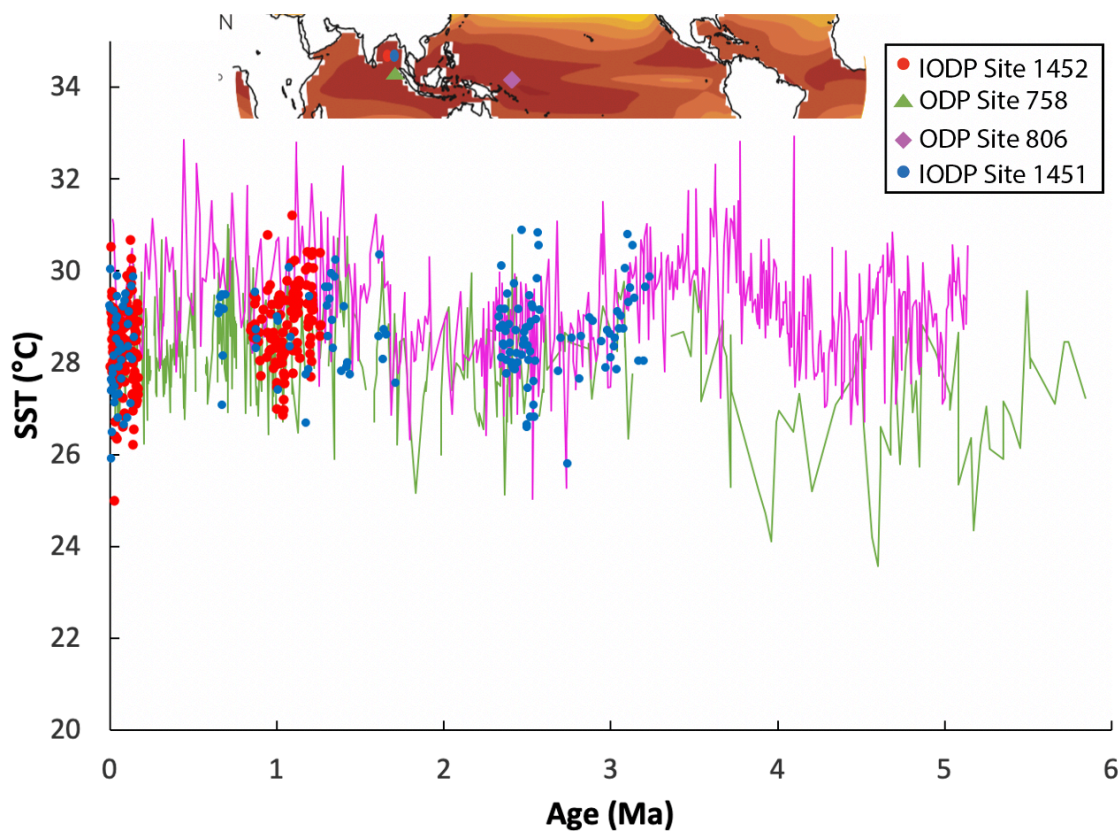


Figure 9 SSTs of our southern Bay of Bengal records compared with those in the tropical Indian Ocean (ODP Site 758; green triangles) and the western equatorial Pacific (ODP 806; purple diamonds). SSTs patterns at Site U1451 are similar to those of ODP Site 758 in the Indian Ocean, and ODP Site 806 in the western Pacific warm pool over the past 3 Ma with average SSTs of 29.1°C, 28.3°C, & 29.6°C respectively.

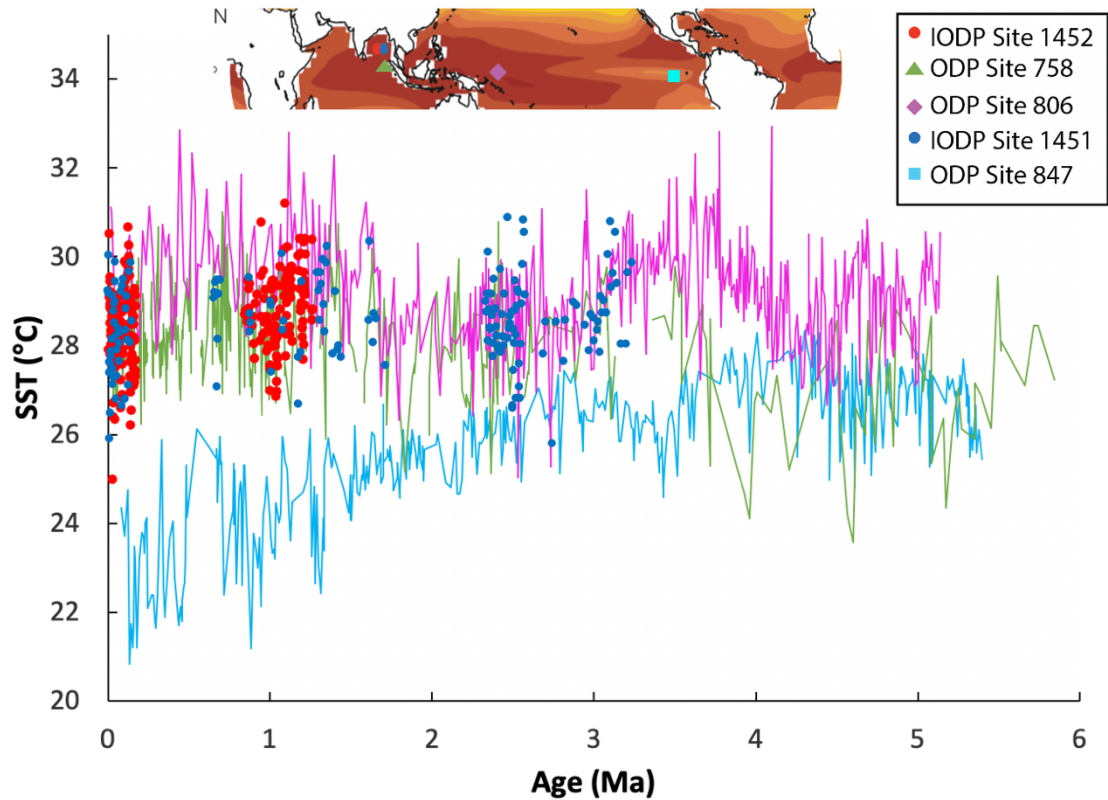


Figure 10 SSTs of our southern Bay of Bengal records compared with those in the tropical Indian Ocean (ODP Site 758; green triangles), the western equatorial Pacific (ODP 806; purple diamonds), and eastern equatorial Pacific (ODP 847; blue squares). SSTs patterns at Site U1451 are similar to those of ODP Site 758 in the Indian Ocean, and ODP Site 806 in the western Pacific warm pool over the past 3 Ma. The eastern equatorial Pacific cools significantly over the past 5 Ma compared to those in the Indo-Pacific Warm Pool.